Nesic, S., Cuerno, R., Moro, E. y Kondic, L. (2015). Fully nonlinear dynamics of stochastic thin-film dewetting. *Physical Review E*, 92(6), 061002(R).

DOI: https://doi.org/10.1103/PhysRevE.92.061002

PHYSICAL REVIEW E **92**, 061002(R) (2015)

Fully nonlinear dynamics of stochastic thin-film dewetting

S. Nesic,[1] R. Cuerno,[1] E. Moro,[1] and L. Kondic[2]
[1]*Departamento de Matemáticas & Grupo Interdisciplinar de Sistemas Complejos (GISC), Universidad Carlos III de Madrid, 28911 Leganés, Spain*
[2]*Department of Mathematical Sciences, New Jersey Institute of Technology, Newark, New Jersey, USA*
(Received 16 May 2015; revised manuscript received 7 August 2015; published 3 December 2015)

The spontaneous formation of droplets via dewetting of a thin fluid film from a solid substrate allows materials nanostructuring. Often, it is crucial to be able to control the evolution, and to produce patterns characterized by regularly spaced droplets. While thermal fluctuations are expected to play a role in the dewetting process, their relevance has remained poorly understood, particularly during the nonlinear stages of evolution that involve droplet formation. Within a stochastic lubrication framework, we show that thermal noise substantially influences the process of droplets formation. Stochastic systems feature a smaller number of droplets with a larger variability in size and space distribution, when compared to their deterministic counterparts. Finally, we discuss the influence of stochasticity on droplet coarsening for asymptotically long times.

DOI: 10.1103/PhysRevE.92.061002 PACS number(s): 47.61.−k, 05.10.Gg, 68.08.Bc, 68.15.+e

The interplay between stochastic fluctuations and nonlinear interactions can induce highly nontrivial effects in spatially extended systems [1] at the nanoscale [2]. For instance, noise can rectify the direction of material transport, as for diffusing particles under asymmetric forces [3]. When a characteristic pattern emerges from a homogenous state [4], fluctuations can even enhance (rather than hinder) spatial order or modify the rate at which typical pattern sizes increase with time (*coarsening*), as e.g. for evolving atomic steps at epitaxial surfaces [5,6].

A natural context in which fluctuations are expected to be relevant is nanoscale fluid flow. Although the (continuum) Navier-Stokes equations remain physically valid down to surprisingly small scales ($\simeq$1 nm) [7,8], the atomistic nature of the fluid medium is expected to play an increasingly important role as physical scales are reduced. In this process the surface-to-volume ratio becomes ever more favorable [9], so that free surface flows [10] provide conspicuous instances for noise effects. Thus, various interfacial processes have been seen to depend critically on the occurrence of fluctuations, such as the breaking of nanojets [11–13] or of liquid threads [14]. In addition, it is known that thermal noise in the fluid velocity field changes the value of the contact angle for partial wetting [15] and enhances the spreading of droplets in surface-tension [16] and gravity [15] driven systems, and the rupture of thin dewetting films [17–19].

Indeed, some dynamical and morphological properties found in dewetting experiments with polymer [20] or liquid metal films [21] remain beyond deterministic frameworks such as the ones employed to describe spinodal dewetting [22]. These formulate the time evolution of coarse-grained quantities, in which microscopic fluctuations have been averaged out. However, the early rupture times and irregular patterns which are experimentally observed suggest that fluctuations play a strong role requiring explicit description. In the long wave (lubrication) approximation to free surface flow [23], such an explicit formulation can be provided by the following a *stochastic* evolution equation for the thickness h of a thin fluid film [16,18],

$$\eta\partial_t h = \partial_x\{(h^3/3)\,\partial_x\big[-\gamma\,\partial_x^2 h - \Pi(h)\big] + \sigma\, h^{3/2}\,\epsilon\}. \quad (1)$$

Here η is viscosity, γ is surface tension, $\epsilon(x,t)$ is a Gaussian white noise of zero mean and unit variance, while the amplitude of the corresponding stochastic term depends explicitly on temperature T as $\sigma = \sqrt{\eta k_B T/3}$. In Eq. (1), $\Pi(h) = -\partial\Phi(h)/\partial h$ is the disjoining pressure that accounts for fluid-solid interaction, with $\Phi(h)$ the interface potential [24]. A power law is commonly used, $\Pi(h) = \kappa[(h_*/h)^n - (h_*/h)^m]$, where κ is proportional to the Hamaker constant and h_* is the precursor film thickness [25,26], corresponding to the minimum of the potential. The balance between surface tension and disjoining pressure sets the equilibrium contact angle [27].

The short-time evolution of dewetting experiments [20] corresponds to the linearized Eq. (1) [19,20]: the destabilizing disjoining pressure, in competition with stabilizing surface tension, induces a morphological instability [4], whereby the film thickness becomes nonhomogeneous in space and surface undulations feature a characteristic size, λ. In a process reminiscent of domain coarsening in phase separation or spinodal decomposition of binary mixtures [28], this size increases nontrivially with time in a form whose description requires large fluctuations [i.e., $\sigma \neq 0$ in Eq. (1)] [20]. However, at these short times the film morphology is still dominated by capillarylike surface modes and differs quite strongly from the expected breakup of the film into distinct droplets. It is not known how large (explicit) thermal fluctuations influence the morphology and evolution of the drop pattern. This includes the very-long-time regime, in which deterministic droplets are expected to undergo coarsening into a single-drop morphology [29,30]. It is natural to ponder whether thermal fluctuations modify the ensuing coarsening law. For instance, explicit noise is known to do so for the one-dimensional (1D) Cahn-Hilliard equation, a paradigmatic model in the context of spinodal decomposition [28,31].

In this Rapid Communication, we study the effect of strong thermal fluctuations on the formation and evolution of droplets under partial wetting conditions. To this end, we study numerically the full time evolution described by Eq. (1), from the earliest times up to late-time coarsening, going into detail through the stochastic nonlinear regime, in which droplets form and nontrivially evolve. Not only do we confirm that

thermal fluctuations speed up the nonlinear process of droplet formation [18], but we also show that fluctuations increase significantly the heterogeneity in droplet sizes and positions inducing disordered droplet patterns, akin to those recently observed [21]. In addition, we also find that while noise accelerates the coarsening that occurs for asymptotically long times [29,30], it does not alter the form of the coarsening law.

To carry out our study, we performed large-scale numerical simulations, in which a scheme like that in [32,33] has been chosen for computational efficiency: To characterize the droplet distribution in space, a large number of droplets (hence, a large domain size L) is required, which is particularly demanding in the presence of noise. Thus, we restrict ourselves to one-dimensional geometry. Our algorithm is based on implicit (Crank-Nicolson) discretization [32], treating surface tension implicitly and $\Pi(h)$ explicitly; we employ zero-flux boundary conditions. The stochastic term is also treated explicitly, the Ito and Stratonovich interpretations having been shown [18] to be equivalent for Eq. (1). Our algorithm implements an adaptive time-stepping procedure whereby positivity-nonpreserving fluctuations are rejected, implying time-step recalculation and noise resampling [32].

We consider a nondimensional version of Eq. (1) by defining $\hat{h} = h/h_c$, $\hat{x} = x/h_c$, and $\hat{t} = t/t_c$, where h_c is a typical film thickness and $t_c = 3\eta h_c/\gamma$. This leads to nondimensional amplitudes $\hat{\sigma} = (k_B T/\gamma h_c^2)^{1/2}$ and to $\hat{\kappa} = \kappa h_c/\gamma$; we use the exponents $(n,m) = (3,2)$ as in, e.g., [27]. The resulting equation looks formally like Eq. (1) with $\eta = \gamma \equiv 1$, but for hatted coordinates and fields. We perform deterministic and stochastic simulations of the nondimensional equation using a precursor thickness $\hat{h}_* = 0.01$ and the same random *initial condition*, namely, random values of the thickness with nondimensional average $\hat{h}_0 = 0.1$ and variance $10^{-2}\hat{h}_0$. The contact angle is set to 50° in the expression $\hat{\kappa} = 2(1 - \cos\theta)/\hat{h}_*$ [27], leading to $\hat{\kappa} = 72$; within the long wave theory implementation, the actual contact angle (measured by the slope of the tangent line passed through the drop profile through the point of inflection) is smaller and is close to 25°. These parameter values are closely related to the polymer films studied in [20], where the characteristic film thickness is 4 nm ($h_c = 40$ nm, so that $\hat{h}_0 = 0.1$), while $\gamma = 0.03$ N/m and the Hamaker constant $A = 2 \times 10^{-20}$ J yield a contact angle in the 15°–20° range. The ensuing nondimensional noise strength $\hat{\sigma} \simeq 10^{-2}$ corresponds to $T = 50$–60 °C. On the other hand, for the liquid metal thin films considered in [21], $\gamma = 1.3$ N/m, $T = 2000$ K, and $h_c \in [50,150]$ nm, leading to $\hat{\sigma} \in [10^{-5/2}, 10^{-3}]$. Finally, the spatial grid size $dx = \hat{h}_*$; such a choice is known to lead to accurate results [32], while the temporal step size is adaptive, as mentioned above. We use a large $L \approx 31\lambda$ value, where λ is the most unstable wavelength obtained by linear stability analysis of the deterministic version of Eq. (1), see below. The number of noise realizations we consider (200) is large enough to obtain significant statistics. We note that preserving non-negativity of solutions to the stochastic equation requires shorter time steps, inducing much longer computation times than deterministic simulations.

Unless otherwise stated, we work in dimensionless units and remove hats for notational simplicity. Figure 1 shows examples of the time evolution predicted by Eq. (1) in the deterministic and stochastic cases. Well-defined droplets (clear bands) emerge after a *rupture time* of roughly $t_{r,det} = 180$ ($t_{r,sto} = 80$) time units in the deterministic (stochastic) system. In the latter case there is a substantial amount of droplet merging around that time, after which activity decreases. Comparing both panels, we immediately observe that the width of the droplets (clear bands) and their locations are much more regular in the deterministic than in the stochastic case.

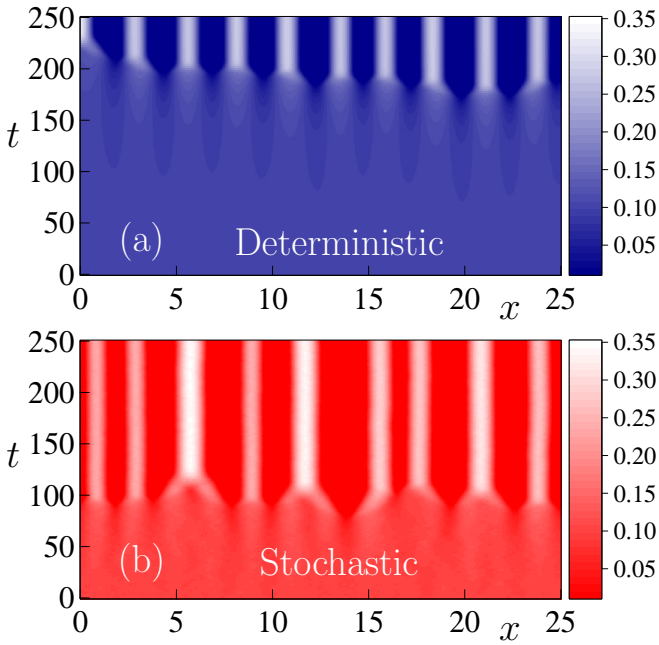

FIG. 1. (Color online) Space-time plot of droplet formation and evolution as predicted by Eq. (1) for $\sigma = 0$ (a) and $\sigma = 10^{-2}$ (b), for the same parameter values and initial conditions, see main text. Brighter (darker) color corresponds to larger (smaller) values of the film thickness $h(x,t)$ according to the color scale on the right of each panel.

Although some spatial modulation can be seen for earlier times in Fig. 1, the system behavior is less visually clear. However, at such times one can resort to linear stability analysis [18,20,27]. The time evolution of the system is conveniently described by the structure factor $S_q = \langle |h_q(t)|^2 \rangle$, which within linear approximation can be analytically obtained [18,20],

$$S_q = (2\pi)^2 \left[S_0(q) e^{2\omega(q)t} + \frac{\sigma^2 h_0^3}{2} \frac{q^2}{\omega(q)} (e^{2\omega(q)t} - 1) \right]. \quad (2)$$

Here, $h_q(t)$ is the Fourier cosine transform [35] of $h(x,t)$ for wave number q, $S_0(q)$ is the initial structure factor, h_0 is a film thickness, and the growth rate is given by the dispersion relation $\omega(q) = h_0^3 q^2 (2q_0^2 - q^2)/3$, where $q_0^2 = -\Pi'(h_0)/2$. The wavelengths of unstable perturbations correspond to $q \in [0, \sqrt{2}q_0]$, for which $\omega(q) \geqslant 0$. Starting from an initial condition with mean h_0, the deterministic system very quickly selects the wave number $q_{m,det} = q_0$ for which the growth rate $\omega(q)$ reaches its positive maximum, see black squares and blue triangles in Fig. 2, where we plot the time evolution of the value of wave number q_m at which the main maximum of S_q occurs. For our parameter choice, $q_0 = 2.464$. Within linear approximation, this sets the length scale of the pattern, $\lambda = 2\pi/q_0 = 2.546$, namely, the average size of surface

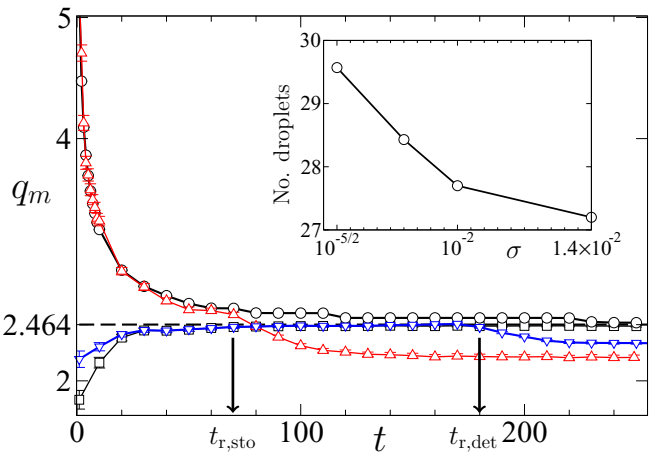

FIG. 2. (Color online) Time evolution of the position of the main maximum, q_m, of the structure factor. The horizontal dashed black line indicates the deterministic linear prediction, q_0. Black circles (squares) correspond to predictions from Eq. (2) for $\sigma = 10^{-2}$ ($\sigma = 0$). Red up (blue down) triangles provide the position of $q_{m,sto}(t)$ [$q_{m,det}(t)$] as obtained in numerical simulations of Eq. (1) for $\sigma = 10^{-2}$ ($\sigma = 0$). Rupture times are signaled by arrows. All results are obtained by averaging over 200 noise realizations. Inset: Number of droplets for different noise amplitudes at $t = 220$. All lines are guides to the eye.

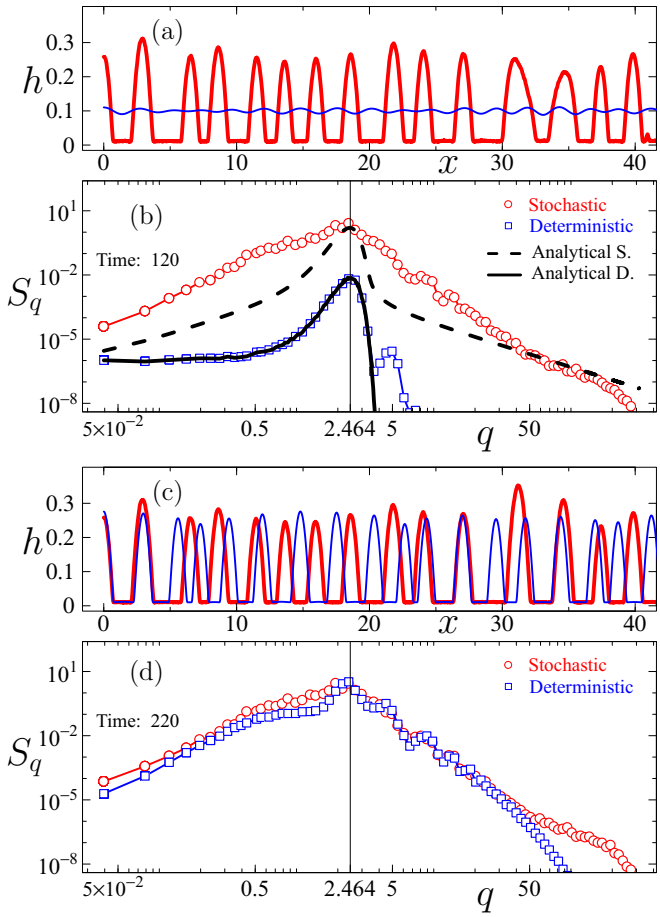

FIG. 3. (Color online) (a), (c): Surface morphologies from simulations of Eq. (1) for $\sigma = 0$ (thin blue line) and $\sigma = 10^{-2}$ (single realization, thick red line) at $t = 120$ (a) and 220 (c). (b), (d): Structure factor averaged over 200 noise realizations, at $t = 120$ (b) and 220 (d) for $\sigma = 0$ (blue squares) and $\sigma = 10^{-2}$ (red circles). The thick black dashed (solid) line in (b) provides the analytical prediction from Eq. (2) for $\sigma = 10^{-2}$ ($\sigma = 0$). Thin solid blue and red lines in (b) and (d) are guides to the eye.

undulations. In contrast, stochastic systems initially develop nontrivial short length scale (large q) correlations, so that $S_q(t)$ displays a maximum for a wave-number value $q_{m,sto}$ which decreases with time towards the deterministic value q_0, see Fig. 2 and [34]. This is the process described in [20] as coarsening. Note that, as mentioned above, droplets have not yet formed; as seen in [34], for these times the film morphology remains largely a small-amplitude sinusoid. In addition, for stochastic simulations, $q_{m,sto} > q_0$; as we will see, this inequality does not hold in the nonlinear regime.

Within the range of validity of the linear approximation, the film develops independent unstable modes. If the linear predictions were applicable to long times, then the number of drops eventually formed would be essentially fixed by the linear value $\lambda = 2.546$, since S_q is characterized by a well-defined peak around $q = q_m$, see thick solid lines in Fig. 3. However, experiments [21] show that the distribution of droplet sizes is relatively wide. Droplets differ strongly from smooth sinusoids, and they interact nontrivially (e.g., through merging and coalescing) during their evolution. Hence, we next need to address droplet formation for times $t \gtrsim 60$, see Fig. 2, away from the linear regime. As seen in the animation provided at [34], nonlinear effects indeed set in for $t \simeq 60$. Thus, the deterministic structure factor develops higher harmonics, while the stochastic S_q also departs clearly from the linear solution, Eq. (2); see Fig. 3 for two sample times. The amplitudes of higher harmonics are at least one order of magnitude smaller than that of the main peak [34], so that they barely influence later stages of the evolution. As seen in linear [19,20] and nonlinear [18] systems, the rupture time at which well-defined droplets form is much shorter for the stochastic ($t_{r,sto} \simeq 80$) than in the deterministic ($t_{r,det} \simeq 180$) case, see [34] and also Fig. 3(a) for $t = 120$, where droplets have appeared in the former case, but not yet in the latter.

After rupture, the S_q distribution broadens around the main peak both in the stochastic and in the deterministic systems, and for values of q on both sides of q_m, see Figs. 3(b) and 3(d) and [34]. Moreover, there is an additional boost in the rupture process so that stochastic droplets create faster than one would expect using the linear theory: Note that rupture times are signaled by a kink in the corresponding $q_m(t)$ data. At rupture, nonlinear ripening of droplets takes place, namely, a decrease of q_m with time, which is more pronounced and occurs earlier in the stochastic system. In contrast to linear predictions, the deterministic system also undergoes a similar, albeit delayed process. We conjecture that disorder in droplet positions favors merging of nearby drops, inducing more rapid decrease of q_m in the stochastic system.

Also, for any $\sigma \geqslant 0$, once the drops are well formed, the decrease in $q_m(t)$ with time slows down. On average, the value of q_m which is eventually achieved (say, for $t \gtrsim 220$) is smaller for $\sigma \neq 0$. This behavior implies a smaller number of drops

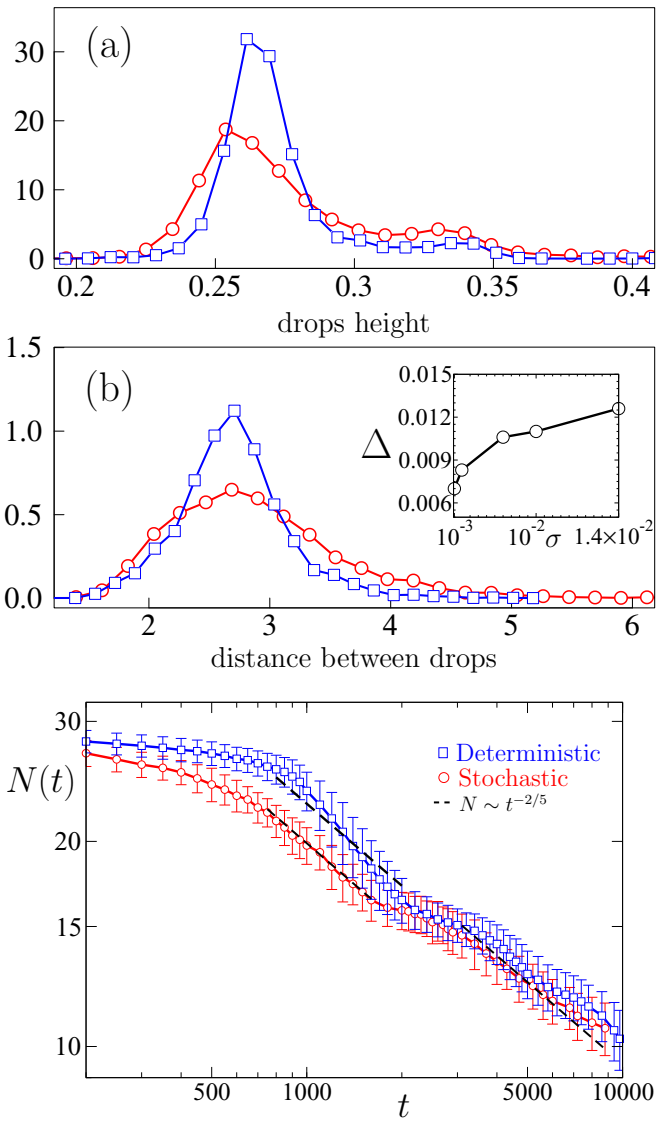

FIG. 4. (Color online) Distribution functions of drop heights (a) and interdrop distances (b) at time $t = 220$ for $\sigma = 0$ (blue squares) and $\sigma = 10^{-2}$ (red circles). Inset: width of the main peak of S_q at $t = 220$, as a function of noise amplitude. Solid black, blue, and red lines are guides to the eye. (c) Number of droplets vs time, $N(t)$, for very long times up to $t = 10\,000$, averaged over 40 noise realizations. We have set $\hat{h}_* = 0.04$ for computational feasibility. Blue squares (red circles) correspond to $\sigma = 0$ ($\sigma = 10^{-5/2}$). The dashed lines correspond to the power-law decay $N(t) \sim t^{-2/5}$ of very large deterministic systems [29]. Solid blue and red lines are guides to the eye.

for a fixed domain in the stochastic system, see e.g. Fig. 3(c). Also recall Fig. 1, where substantial drop merging is seen for this case during times from rupture up to $t \simeq 120$. We note that for the time scales considered so far, the final number of droplets decreases when the noise intensity (say, temperature) increases, see the inset of Fig. 2.

Figures 4(a) and 4(b), showing the distribution of drop heights and their distances, illustrate a further significant difference between stochastic and deterministic evolution: Stochasticity indeed leads to much wider droplet distributions, and therefore to much more irregular patterns. Two sample morphologies are compared in Fig. 3(c). Also, the inset in Fig. 4(b) shows that the width at half maximum of the S_q distribution, Δ, is an increasing function of noise amplitude, as expected. This finding may be of significant importance in applications where regularity of the distribution of drops is often desired. Our results suggest that decreasing noise amplitude may be the key to achieving this goal.

On still longer time scales, the number of drops needs to further reduce: Indeed, the stochastic Eq. (1) drives the system to an equilibrium state at temperature T in which height configurations follow the Boltzmann distribution $\mathcal{P}\{h\} \propto e^{-\mathcal{H}/k_B T}$, with effective interface Hamiltonian $\mathcal{H}[h] = \int dx\,[\Phi(h) + \gamma(\partial_x h)^2/2]$ [18,25]. Since one larger drop is energetically more favorable than two smaller ones [29], a single droplet is the stable configuration that will be reached by the system with the highest probability as a result of a coarsening process. Thus, although the asymptotic state is the same as for the deterministic system [29], in principle the rate of convergence needs not be the same, as thermal fluctuations can help the system surpass local energetic barriers. Returning to our simulations, up to the times discussed so far, the decrease of $q_m(t)$ seems mostly induced by droplet coalescence. This introduces relatively large distances among remaining units, recall Fig. 1 for $t \gtrsim 200$. For still longer times, droplet interaction occurs mostly through the precursor layer, indeed inducing noninterrupted coarsening of the pattern into a single drop morphology [29]. For well-separated droplets and $\sigma = 0$, analytical predictions actually exist for the decrease of the number of droplets $N(t)$ with time [29]. We have considered the evolution predicted by Eq. (1) for $\sigma \neq 0$ at very long times, up to $t = 10^4$. Computational feasibility requires a larger precursor thickness $h_* = 0.04$ and smaller noise, $\sigma = 10^{-5/2}$. Our results indicate that fluctuations do shorten significantly the time scales on which coarsening occurs. However, they become less relevant with increasing time, to the extent that the asymptotic behavior of $N(t)$ is not modified with respect to the deterministic case, at least within the accuracy of the results, see Fig. 4(c) and [36]. Thus, droplet coarsening counts among phenomena for which noise does not change the coarsening universality class [28] of the corresponding deterministic system.

In summary, we have shown that stochastic effects due to strong thermal noise may play a significant role in dewetting of thin fluid films, in each of the three stages of evolution considered. For very early times, as predicted by linear theory [19,20], stochasticity leads to a decrease of the most unstable wave number, $q_{m,sto}$, down from the values that are large compared to the deterministic one, q_0; however, within this stage $q_{m,sto}$ remains larger than q_0. After this, noise triggers an earlier onset of nonlinear effects inducing, as anticipated [17], a shorter rupture time [18]. At these time scales stochasticity leads to droplet coarsening, in the sense that $q_{m,sto} < q_0$, in contrast to the linear regime. The ensuing pattern is heterogeneous both in individual droplet features (heights, widths) and in interdroplet distances. Finally, for much longer times, fluctuations speed up the coarsening process that will ultimately lead to formation of the single-drop, energetically favored state. Qualitatively, the deterministic coarsening law for the number of drops remains unchanged. However, *quantitatively*, the time scales involved in this long-time coarsening process are significantly

influenced by noise, and we conjecture that stochastic effects may be observable in careful experiments carried out with fluid films of nanoscale thickness. In this respect, note that our present results have been obtained for a 1D system. In the process of generalizing our results to the 2D case, it would be extremely important to verify if behavior may turn out to be similar to that of the paradigmatic Cahn-Hilliard (CH) equation. Indeed, while noise has a similar accelerating role as in our case with respect to the domain coarsening properties of the 1D deterministic equation [37], it is expected to have a less relevant role in 2D [38]. Some, e.g., topological, differences between the deterministic and stochastic systems seem nevertheless to persist in the latter case [39,40]. It would be extremely interesting to consider the full 2D case for Eq. (1) in detail, and thus understand the role of dimensionality on the relevance of stochastic effects.

Partial support for this work was provided by MINECO (Spain) Grants No.FIS2010-22047-C05-04 and No.FIS2012-38866-C05-01, and by NSF (USA) Grant No. CBET-1235710. S.N. acknowledges support by Universidad Carlos III de Madrid.

[1] F. Sagués, J. M. Sancho, and J. García-Ojalvo, Rev. Mod. Phys. **79**, 829 (2007).
[2] U. Landman, Proc. Natl. Acad. Sci. USA **102**, 6671 (2005).
[3] P. Hänggi and F. Marchesoni, Rev. Mod. Phys. **81**, 387 (2009).
[4] M. C. Cross and H. S. Greenside, *Pattern Formation and Dynamics in Nonequilibrium Systems* (Cambridge University, Cambridge, UK, 2009).
[5] P. Politi, G. Grenet, A. Marty, A. Ponchet, and J. Villain, Phys. Rep. **324**, 271 (2000).
[6] C. Misbah, O. Pierre-Louis, and Y. Saito, Rev. Mod. Phys. **82**, 981 (2010).
[7] L. Bocquet and E. Charlaix, Chem. Soc. Rev. **39**, 1073 (2010).
[8] F. Detcheverry and L. Bocquet, Phys. Rev. E **88**, 012106 (2013).
[9] D. L. Allara, Nature **437**, 638 (2005).
[10] R. V. Craster and O. K. Matar, Rev. Mod. Phys. **81**, 1131 (2009).
[11] M. Moseler and U. Landman, Science **289**, 1165 (2000).
[12] J. Eggers, Phys. Rev. Lett. **89**, 084502 (2002).
[13] Y. Hennequin, D. G. A. L. Aarts, J. H. van der Wiel, G. Wegdam, J. Eggers, H. N. W. Lekkerkerker, and D. Bonn, Phys. Rev. Lett. **97**, 244502 (2006).
[14] J. Petit, D. Riviere, H. Kellay, and J.-P. Delville, Proc. Natl. Acad. Sci. USA **109**, 18327 (2012).
[15] S. Nesic, R. Cuerno, E. Moro, and L. Kondic, Eur. Phys. J. ST **224**, 379 (2015).
[16] B. Davidovitch, E. Moro, and H. A. Stone, Phys. Rev. Lett. **95**, 244505 (2005).
[17] J. Becker, G. Grün, R. Seemann, H. Mantz, K. Jacobs, K. R. Mecke, and R. Blossey, Nat. Mater. **2**, 59 (2003).
[18] G. Grün, K. Mecke, and M. Rauscher, J. Stat. Phys. **122**, 1261 (2006).
[19] K. Mecke and M. Rauscher, J. Phys. Condens. Matter **17**, S3515 (2005).
[20] R. Fetzer, M. Rauscher, R. Seemann, K. Jacobs, and K. Mecke, Phys. Rev. Lett. **99**, 114503 (2007); M. Rauscher and S. Dietrich, Annu. Rev. Mater. Res. **38**, 143 (2008).
[21] A. G. González, J. A. Diez, Y. Wu, J. D. Fowlkes, P. D. Rack, and L. Kondic, Langmuir **29**, 9378 (2013).
[22] A. Sharma, C. S. Kishore, S. Salaniwal, and E. Ruckenstein, Phys. Fluids **7**, 1832 (1995); A. Sharma, Eur. Phys. J. E **12**, 397 (2003).
[23] A. Oron, S. H. Davis, and S. G. Bankoff, Rev. Mod. Phys. **69**, 931 (1997).
[24] H.-J. Butt, K. Graf, and M. Kappl, *Physics and Chemistry of Interfaces* (Wiley-VCH, Weinheim, 2003).
[25] V. Mitlin, J. Colloid Interface Sci. **227**, 371 (2000).
[26] D. Bonn, J. Eggers, J. Indekeu, J. Meunier, and E. Rolley, Rev. Mod. Phys. **81**, 739 (2009).
[27] J. A. Diez and L. Kondic, Phys. Fluids **19**, 072107 (2007).
[28] A. J. Bray, Adv. Phys. **43**, 357 (1994).
[29] K. B. Glasner and T. P. Witelski, Phys. Rev. E **67**, 016302 (2003); Physica D **209**, 80 (2005).
[30] R. Limary and P. F. Green, Langmuir **19**, 2419 (2003).
[31] A. Torcini and P. Politi, Eur. Phys. J. B **25**, 519 (2002).
[32] J. A. Diez, L. Kondic, and A. Bertozzi, Phys. Rev. E **63**, 011208 (2000).
[33] L. Zhornitskaya and A. L. Bertozzi, SIAM J. Numer. Anal. **37**, 523 (1999).
[34] See Supplemental Material at http://link.aps.org/supplemental/10.1103/PhysRevE.92.061002 for a movie showing $h(x,t)$ and $S_q(t)$ for times $t \in [1,250]$, together with the histograms of individual drop heights and interdrop distances, for deterministic and stochastic simulations of Eq. (1).
[35] J. P. Boyd, *Chebyshev and Fourier Spectral Methods* (Dover, New York, 2001).
[36] See Supplemental Material at http://link.aps.org/supplemental/10.1103/PhysRevE.92.061002 for a movie with the evolution of $h(x,t)$ for parameters and times as in Fig. 4(c).
[37] K. A. Hawick, in *Proceedings of the IASTED International Conference on Modeling, Identification and Control (MIC'10)* (IASTED, Phuket, 2010), p. 33.
[38] C. Castellano and S. C. Glotzer, J. Chem. Phys. **103**, 9363 (1995).
[39] M. Gameiro, K. Mischaikow, and T. Wanner, Acta Mater. **53**, 693 (2005).
[40] D. Blömker, S. Maier-Paape, and T. Wanner, Trans. Am. Math. Soc. **360**, 449 (2008).